# Network Formation without Vitrification Limitation: Ring-Opening Polymerization of Sulfonium Zwitterion Monomers

**Loren W. Hill,*,† Nelson Rondan,‡ and Donald Schmidt‡**

*Coatings Consultant, 9 Bellows Road, Wilbraham, Massachusetts 01095; and The Dow Chemical Company, Midland, Michigan 48674*

*Received September 26, 2000; Revised Manuscript Received November 10, 2000*

ABSTRACT: Thermal cure of zwitterion monomers resulted in films having a glass transition temperature, $T_g$, that was 75 °C higher than the cure temperature. It was concluded that zwitterion cure is not limited by vitrification. Molecular modeling of the dimer complex indicated a preferred conformation in which reactive groups on adjacent monomer molecules are situated close to each other. Absence of vitrification limitation is attributed to the possibility of reaction with very little movement. Dynamic mechanical analysis (DMA) was used to determine $T_g$ and to indicate cross-link density.

## I. Introduction

Gillham[1] and others[2] have shown that conversion of functional groups during network formation by condensation of polyfunctional monomers ceases or slows greatly when the glass transition temperature of the forming network has risen to the temperature of cure, $T_{cure}$. Lack of segmental mobility is believed to prevent reacting groups from coming close together in the incipient glassy state which prevents bimolecular reaction. One result is the presence of unconverted functional groups in the glassy film. If the partly cured thermoset is subsequently heated to a temperature higher than the original cure temperature, the unconverted groups become mobile again and the interrupted reaction begins again. Of course the $T_g$ increases again as groups are converted, but when all of the groups have been converted, there is no further rise in $T_g$. The value of $T_g$ at complete conversion is called $T_{g,max.}$ The effects of vitrification on thermoset cure are ubiquitous. The authors could not find any examples in the literature for which the vitrification limitation was avoided. In the present work, however, observation of extreme hardness with low cure temperatures and the relationship between $T_g$ and $T_{cure}$ suggest that cure response of zwitterion ion monomers is not limited by vitrification.

Aryl cyclic sulfonium zwitterions (ACS zwitterions)[2−7] have structures with a cyclic sulfonium ion attached through the sulfonium sulfur to a phenolic aromatic ring. Upon heating, these zwitterions polymerize by a mechanism involving nucleophilic attack of the phenolic anion on the ring carbon adjacent to the sulfonium sulfur (eq 1). Polymerization occurs by ring opening and

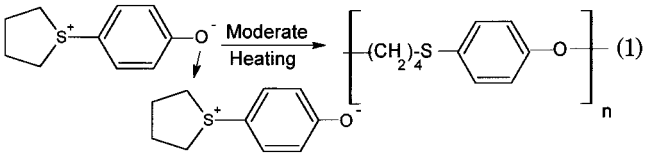


(1)

loss of charge. Polyfunctional ACS zwitterions yield highly cross-linked coatings.[8] Use of photolytic cross-linking of ACS zwitterions has been described recently for microelectronics with water as a developer.[9] The ACS zwitterions obtained by functionalizing bisphenol A, structure **1**, yield an exceptionally hard, tough adherent coating.[10]

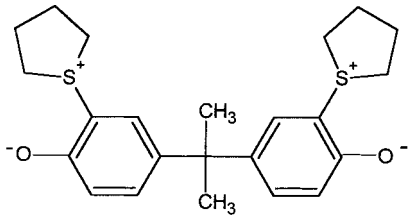


**1**

Molecular modeling of monomer molecules and of the dimer complex of ACS zwitterions has been used to clarify the reactive site orientation. The reactive site orientation is shown to be favorable for reaction.

## II. Experimental Section

**Preparation of Bisphenol ACS Zwitterion 1,1-[Isopropylidenebis(6-hydroxy-*m*-phenyl)]bis(tetrahydrothiophenium hydroxide) Bis(inner salt). *Caution*!** Because of the hazardous nature of this synthesis,[11] only highly trained people using the proper safety equipment (gloves, goggles, respirator, etc.) should attempt to prepare this compound. All operations must be carried out in an efficient hood, and the hazardous waste must be disposed of properly. The glass equipment and starting materials should be dry.

A three-neck, ball joint 1000-mL flask (Ace Glass, Vineland, NJ, #6950) is equipped with the following: Trubore stirrer (#8051−35), Claisen adaptor (#5060), thermometer and adapter (#8300), and dry ice condenser (Dewar type #5964). A slight positive pressure of nitrogen is maintained by using a mineral oil bubbler (#8761) connected to a T-type connector (#12513) and dry nitrogen source. The acid gases are absorbed using a packed gas absorbent tower (column) and circulating NaOH solution as described elsewhere.[12]

With the stirrer running, sulfur dioxide (309 g, 209 mL) is condensed through an attached dry ice-cooled condenser and collected in a three-necked flask cooled with dry ice/2-propanol bath. Tetrahydrothiophene (85 g, 0.964 mol, 85 mL) and iodine (10 mg) are added. Hydrogen chloride gas (22 g) is slowly introduced while the stirrer is running. The oil bubbler is used as an indicator of the rate of absorption of HCl, and the flow of HCl is adjusted accordingly. Sulfuryl chloride $SO_2Cl_2$ (125 g, 74.4 mL, 0.926 mol) is added dropwise slowly enough to keep the temperature below −40 °C. Bisphenol A (Aldrich, 99+ %,

† Coatings Consultant.
‡ The Dow Chemical Co.

10.1021/ma001674x CCC: $20.00 
Published on Web 12/08/2000

100 g, 0.438 mol) is added, the cooling bath is subsequently removed, and the reaction ingredients are allowed to reflux at −10 °C. After 4 h the dry ice bath and dry ice condenser are removed, and a room-temperature water bath is placed under the reaction flask. The escaping acid gas is directed into the absorbent column.[12] After about 1 h, the temperature has increased to 10 °C, and 1 g of water is slowly added dropwise to the clear, stirred, viscous solution. Nitrogen is then purged across the solution, and the water bath temperature is increased to about 45−50 °C to drive more evolving gases into the absorbent column. After about 190 min viscosity has increased, and 350 mL of methyl ethyl ketone is added. Aspirator vacuum is applied and controlled by bleeding in air to keep the solution material from bubbling out of the flask. The removal of vapor is continued until solids precipitate. The stirrer is stopped, and the off-white solids are collected on a sintered glass filter and washed four times with methyl ethyl ketone. The solid is immediately dried in a hood by spreading on paper to obtain free-flowing powder. The off-white solid at this point is relatively unstable and cannot be stored at ambient temperature. The solid is dissolved in 1 L of 50/50 volume ratio of water/methanol. Dowex SBR−OH ion-exchange resin (The Dow Chemical Co., Midland, MI) is added to the solution with stirring until the pH increases to 10.4. The ion-exchange resin is removed by filtration and rinsed with methanol to recover the residual product. Sufficient solvent is removed under vacuum to yield 467 g of about a 30 wt % solution of zwitterion monomer (79% yield). The solution should be refrigerated or frozen to increase shelf life.

**Film Preparation and Dynamic Mechanical Analysis (DMA).** Aqueous solutions of the BPA ACS Zwitterion were draw coated with a doctor blade on a metal plate coated with a release coating. The films were air-dried for 20 min and then oven cured for 1.5 h at 82 or 164 °C. The cured film was carefully peeled off the low energy surface substrate, and 0.4 × 3.0 cm strips were die cut to prepare samples for DMA. DMA was carried out on films of 30 $\mu$m thickness on an Autovibron (Imass Inc.) at 11 cycles per second oscillating frequency with a temperature scan rate of 2 °C/min. Details of the DMA method used here have been described.[13]

**Computational Methods.** The geometries of the zwitterion monomer and the dimer complex were optimized using the ab initio method and the 6-31G* basis set[14] contained in the SPARTAN program.[15] The optimized geometries were obtained for the monomer and for the dimer complex. The electrostatic potential for the zwitterion monomer was generated using the SPARTAN program and was displayed graphically by color. (The electrostatic potential is calculated as the energy of interaction of a point positive charge with the nuclei and electrons of a molecule. If the point positive charge sees an electron poor region the interaction is repulsive such that the resulting electrostatic potential is positive and is depicted graphically in blue. If the point positive charge is placed in an electron rich region the interaction is attractive. Consequently, the resulting electrostatic potential is negative and depicted in red. If one moves the point positive charge around the molecule an electrostatic potential map is generated.)

## III. Results and Discussion

**DMA of Cured Films.** DMA has been used extensively to study the extent of cure of thermoset industrial coatings.[13] Cured samples are often analyzed as free films with tensile deformation at very low values for the maximum oscillatory strain, $\epsilon_o$. For example, in this work, $\epsilon_o$ was just 0.2%. The sample neither breaks nor yields with such low strain, which facilitates obtaining dynamic properties such as storage modulus ($E'$) and loss tangent (tan $\delta$) over a wide temperature range during a single scan. Films prepared from BPA sulfonium zwitterion monomer with a cure temperature of 82 °C were analyzed by DMA over the temperature range of −20 to +300 °C.

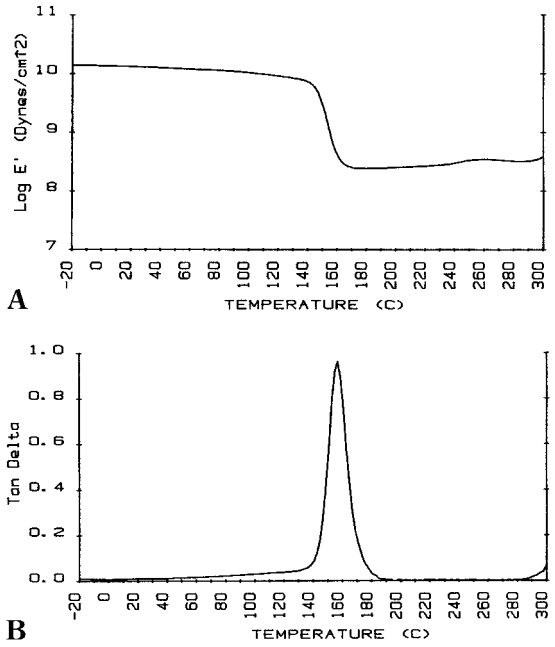


**Figure 1.** DMA plots for BPA ACS zwitterion films cured for 1.5 h at 82 °C: (A) storage modulus ($E'$) vs temperature; (B) loss tangent vs temperature.

The $E'$ vs temperature plot is shown in Figure lA. $E'$ remains nearly constant throughout the glassy region from −20 to about +150 °C where a sharp drop in modulus is observed. The drop in modulus is attributed to the glass transition. Beyond 160 °C, the modulus is again quite constant in a region referred to as the rubbery plateau. The glass transition is clearly very sharp occurring in the 150−160 °C range. Sharp transitions, as observed here, indicate that the network has a highly uniform structure.[13] As noted in the Introduction, ACS zwitterions are reported[8] to yield highly cross-linked coatings. Results of Figure lA are consistent with high cross-link density in the network structure. Values of $E'$ at temperatures above the glass transition are reported to be proportional to cross-link density of short chain networks.[16] The value of $E'$(min) in Figure lA (2.4 × $10^8$ dyn/cm$^2$) is similar to the values observed for highly cross-linked acrylic automotive topcoats.

The loss tangent vs temperature plot is shown in Figure 1B. The value of $T_g$ is often taken as the temperature of the maximum in the tan $\delta$ plot.[13] For Figure 1B the value of $T_g$ is 157 °C based on the tan $\delta$ maximum. This value is remarkably high for a film cured at the much lower temperature of 82 °C. As noted in the Introduction,[1,2] the vitrification limitation holds that $T_g$ cannot rise significantly above $T_{cure}$, but for the BPA zwitterions films of Figure 1B, $T_g$ is 75 °C higher than $T_{cure}$. One possible explanation for this finding is that the $T_g$ is not this high in the originally cured material but increases during the DMA temperature scan. In study of thermoset systems generally,[13] use of temperature scanning techniques sometimes gives an inaccurate indication of initial $T_g$ because the $T_g$ is driven upward as the temperature is increased in a process called "chasing".[13] For the experiment described in Figure 1B, it is not likely that chasing is occurring because the tan $\delta$ peak is so symmetrical. When chasing takes place, the low temperature side of the tan $\delta$ peak has a significantly lower slope than the high-temperature side. For the experiment described in Figure 1B, the tan $\delta$ peak is very symmetrical.

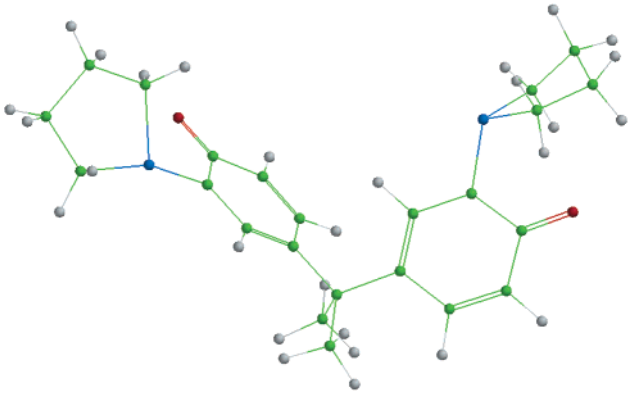

**Figure 2.** Optimized structure of the monomer according to the 6-31G* basis set.

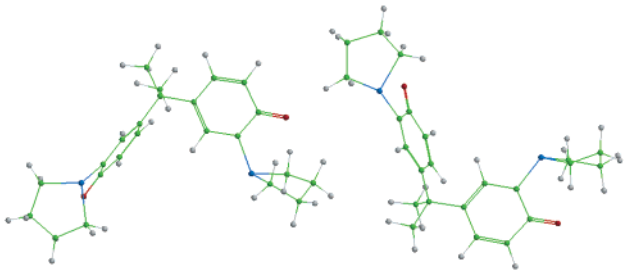

**Figure 3.** Computed structure of the zwitterionic dimer according to the 6-31G* basis set.

**Molecular Modeling.** Molecular modeling of the zwitterion monomer gave the optimized geometry shown in Figure 2. In the preferred conformation about the sulfur atom (blue), the phenolate plane bisects the five membered ring. From bond lengths in the computed structure we can see that the phenolate moiety adopts a "quinoid" structure. The C−O (1.24 Å) and aromatic C−S (1.73 Å) bonds possess double bond character. Furthermore, the C−C bonds of the aromatic ring are not equal in length but instead have some alternating single and double bond character. These features indicate some contribution by a resonance form that has ylide characteristics (structure **2**). Structure **2** has no

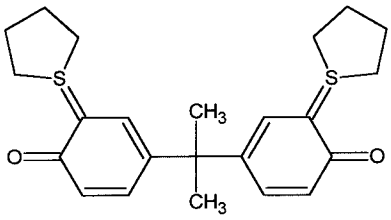


**2**

formal charges whereas the resonance form shown previously (structure **1**) emphasizes the ionic nature of the zwitterion monomer.

A plausible explanation for absence of vitrification limitation is that ionic monomer units align so that reaction can occur without significant segmental motion. Alignment was studied by molecular modeling of the dimer complex. The optimized structure of the dimer complex is shown in Figure 3. The stabilization energy of the dimer complex relative to two isolated monomer units is 6.2 kcal/mol according to the 6-31G* basis set. In eq 1 shown previously, the proposed polymerization mechanism depicted nucleophilic attack by the phenolate oxygen atom on the methylene group adjacent to the ring sulfur atom. In the optimized structure of the dimer complex (Figure 3), the distance between the nucleophilic oxygen and the electrophilic $-CH_2-$ moiety is only 3.3 Å. These sites are primed for reaction. We believe this geometry explains the absence of a vitrification limitation.

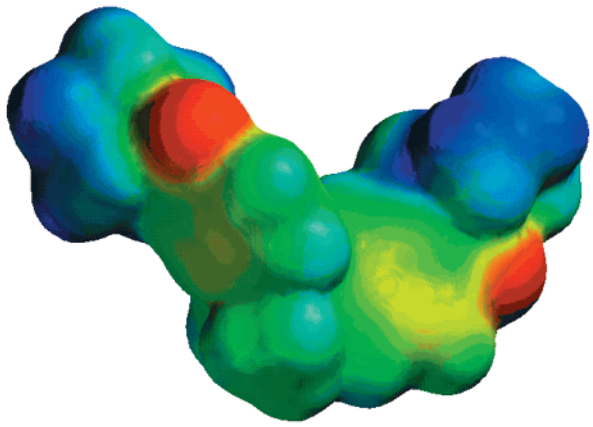

**Figure 4.** Computed electrostatic potential of the zwitterionic monomer according to the 6-31G* basis set.

Including preparation of an electrostatic potential map as part of molecular modeling can contribute to establishing reaction mechanism. The computed electrostatic potential of the zwitterion monomer is shown in Figure 4. As described under computational methods, an electron rich region will appear red and an electron poor region will appear blue. In agreement with the proposed mechanism, the most nucleophilic site on the monomer is revealed to be the phenolate oxygen atom with a minus one formal charge in structure **1** ($-O^-$, depicted as red in Figure 4). The electrophilic site, however, is the $-CH_2-$ moiety (shown in blue) adjacent to the sulfur.

**DMA of Films Cured at 164 °C.** Zwitterion films of Figure 1 were cured at 82 °C, but to check for completion of cure a second series was cured at 164 °C for 1.5 h. DMA results are compared in Figure 5. $E'$ plots (Figure 5A) are similar for the two films in the glassy region and in the transition region. These results suggest that the lower cure temperature does not reduce the extent of the cure significantly compared to the cure obtained at the higher temperature. Rather surprising results are observed in the rubbery plateau region where the film cured at 82 °C has a higher $E'$ plateau value than the one cured at 164 °C. This finding indicates that the cross-link density is higher for the lower cure temperature. It appears likely that at 164 °C, the film cures completely rather quickly, but then cross-links are lost during the later stages of the 1.5 h cure time. The film cured at 82 °C may also cure completely, but the lower temperature decreases the tendency to undergo loss of cross-links. Another possible explanation is that the higher cure temperature might favor intramolecular cyclization leading to lower cross-link density.

Loss tangent plots are compared for the two cure temperatures in Figure 5B. It is obvious that the two peaks occur at very near the same temperature, 157 and 158 °C, which are the same within response variation. This finding is strong evidence that the alignment of ionic groups in monomeric complexes favor reaction without the need for segment mobility. The peaks are both very symmetrical which argues against the chasing effect discussed above. The tan $\delta$ peak is higher for the

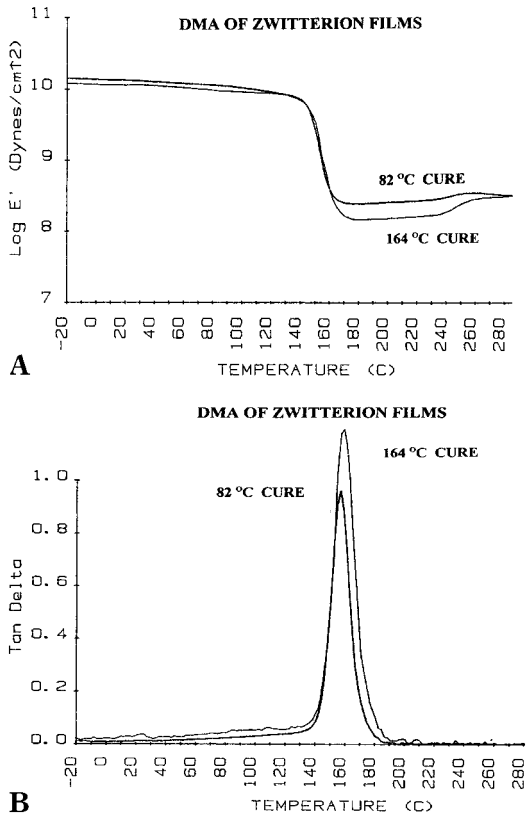


**Figure 5.** (A) Storage modulus plots for zwitterion films cured at 82 or 164 °C for 1.5 h. (B) Loss tangent plots for zwitterion films cured at 82 or 164 °C for 1.5 h.

higher cure temperature. This indicates that greater viscous flow is possible during the transition. Greater viscous flow in the transition could result from lower cross-link density at 164 °C cure for reasons discussed previously. In general, a low peak height is associated with higher extent of cure.[13] Therefore, the higher peak (Figure 5B) and the lower plateau modulus (Figure 5A) at 164 °C are both consistent with the same effect, which is believed to be lower cross-link density at the higher cure temperature.

Penetration hardness (Tukon, ASTM D 1474) was also determined for zwitterion films. Films were very hard even when cured at moderate temperature. For example, the Tukon hardness of a film cured at 85 °C was determined to be 23 KHN (Knoop hardness number) at a dry film thickness of 0.83 mil (21 $\mu$m). For comparison, it can be noted that various automotive topcoats give values in the range 8−12 KHN.

## IV. Conclusions

DMA results and hardness development during thermal cure indicate that cure of zwitterion monomers is not limited by vitrification. In one case, we observed that a zwitterion film had a $T_g$ value that was 75 °C higher than $T_{cure}$. Furthermore, $T_g$ was found to be independent of cure temperature. Molecular modeling of the zwitterion monomer showed the electrostatic potential of various atoms. The position of nucleophilic attack in the proposed polymerization mechanism was consistent with the computed potential. Modeling of the dimer complex showed the favored spatial arrangement of reactive groups. Reactive groups on adjacent molecules were close to each other in the favored dimer geometry. Absence of vitrification limitations is attributed to a geometry in which reactive sites on neighboring monomer molecules are primed for reaction.

## References and Notes

(1) Gillham, J. K. *Polym. Int. J.* **1997**, *44*, 262−276.
(2) Wicks, Z. W., Jr.; Jones, F. N.; Pappas, S. P. *Organic Coatings Science and Technology*, 2nd ed.; Wiley-Interscience: New York, 1999; p 219.
(3) Hatch, M. J.; Yoshimine, M.; Schmidt, D. L.; Smith, H. B. *J. Am. Chem. Soc.* **1971**, *93*, 4617.
(4) Schmidt, D. L.; Smith, H. B.; Yoshimine, M.; Hatch, M. J. *J. Polym. Sci.* **1972**, *A-1, 10*, 2951.
(5) Schmidt, D. L. In *Ring Opening Polymerization*; Saegusa, T., Goethals, E., Eds.; ACS Symposium Series; American Chemical Society: Washington, DC, 1977; p 318.
(6) Gunatillake, P.; Odian, G.; Schmidt, D. L. *Macromolecules* **1985**, *19*, 1779.
(7) Gunatillake, P.; Odian, G.; Schmidt, D. L. *Macromolecules* **1989**, *21*, 1556.
(8) Schmidt, D. L.; Smith, H. B.; Broxterman, W. E. *J. Paint Technol.* **1974**, *46* (588), 41.
(9) So, Y.-H.; Schmidt, D. L.; Bishop, M. T.; Miller, D. R.; Smith, P. B.; Radler, M. J.; Magyar, M.; Kaliszewski, B. L. *J. Polym. Sci., Part A: Polym. Chem.* **2000**, *38*, 1283.
(10) Klingler, T. C.; Schmidt, D. L.; Jensen, W., Jr.; Urchick, D. U.S. Patent 4 089 887, 1978.
(11) Schmidt, D. L.; Heeshen, J. P.; Klingler, T. C.; McCarthy, L. P. *J. Org. Chem.* **1985**, *50*, 2840. (See also: D. L. Schmidt, N. E. Skelly, U.S. Patent 4 968 433, 1990.)
(12) Peters, M. S., Timmerhaus, K. D., Eds. *Plant Design and Economics for Chemical Engineers*; McGraw-Hill: New York, 1980; p 748−750.
(13) Hill, L. W. In *Paint and Coating Testing Manual*, 14th ed.; Koelske, J. V., Ed.; ASTM Manual Series, MNL 17; Am. Soc. for Testing Materials: Philadelphia, PA, 1995; pp 534−546.
(14) Hariharan, P. C.; Pople, J. A. *Chem. Phys. Lett.* **1972**, *66*, 217.
(15) SPARTAN is a product of Wavefunction, Inc., 18401 Von Karman Avenue, Suite 370, Irvine, CA 92715.
(16) Hill, L. W. *Prog. Org. Coat.* **1997**, *31*, 235.

MA001674X